Received: 7 April 2023 | Revised: 17 January 2024 | Accepted: 7 February 2024

DOI: 10.1049/rpg2.12967

IET Renewable Power Generation

The Institution of Engineering and Technology WILEY

ORIGINAL RESEARCH

Grid-forming converters in interconnected power systems: Requirements, testing aspects, and system impact

Soenke Rogalla[1] | Philipp Ernst[1] | Hendrik Lens[2] | Thomas Schaupp[3] | Christian Schöll[2,3] | Roland Singer[1] | Jakob Ungerland[1]

[1]Fraunhofer Institute for Solar Energy Systems ISE, Freiburg, Germany

[2]IFK, University of Stuttgart, Stuttgart, Germany

[3]TransnetBW, Stuttgart, Germany

Correspondence
Soenke Rogalla, Fraunhofer Institute for Solar Energy Systems ISE, Heidenhofstr. 2, 79110 Freiburg, Germany.
Email: soenke.rogalla@ise.fraunhofer.de

Funding information
German Federal Ministry for Economic Affairs and Climate Action, Grant/Award Number: FKZ 0350015A-D

Abstract

In this study, the integration of grid-forming (GFM) converters in power systems is discussed in terms of both the fundamental aspects of system stability and the technical possibilities of converter-based resources. The paper provides a survey and comparison of various GFM control concepts with respect to their transient and stationary behavior. A method for black box characterization and conformity testing of GFM converters is presented and relevant results of lab and field tests with GFM converters are discussed. Finally, important system aspects are addressed. This includes an approach to consider the behavior of GFM converters in distribution grid models and investigations on the minimum share of GFM units required to ensure system stability. The findings of this paper provide valuable insights for the design and implementation of GFM converters in modern converter-based power systems.

1 | INTRODUCTION

The global energy transition towards sustainable and renewable energy sources is leading to a paradigm shift in the way how stability of power systems is ensured. To date, synchronous machines (SM), mostly installed in large conventional power plants, provide the fundamental characteristics that form the basis for grid control and stability mechanisms of interconnected systems. This covers basically the ability to regulate the system voltage and frequency, to provide inertia and damping, and to deliver short-circuit current [1]. In modern converter-based power systems, grid stability must be ensured even when converter-based resources cover up to 100% of the generation. Consequently, future converters must provide all features necessary for grid stability and control. Converters that are capable of this are referred to as *grid-forming* (GFM); in contrast to *grid-following* (GFL) converters used today, which are designed to feed in current after having synchronized to a given grid voltage.

However, integrating GFM converters into power systems is not just a matter of replacing the converter's current controller with a voltage controller. All aspects of power system dynamics must be considered to design a suitable behavior of GFM converters. This is necessary to fully replace the grid stabilizing properties of SM with converters.

The basic concepts for GFM converters were developed back in the 1990s. At that time, the focus was on battery converters for PV/Diesel microgrids on a kilowatt-scale [2]. Droop-based concepts already allowed communication-free parallel operation of voltage-controlled inverters [3]. Meanwhile, a variety of different GFM control concepts have emerged that attempt to mimic the fundamental behavior of SM. The survey paper [4] provides an overview of the most discussed concepts.

Nowadays, system needs of large interconnected systems are the drivers for the development and the design of GFM converters [5–7]. In 2020, the ENTSO-E Technical Group on High Penetration of Power Electronic Interfaced Power Sources (HPoPEIPS) released a report stating that converters are characterized as GFM if they can create system voltage, contribute to fault level, act as a sink for harmonics and unbalances, contribute to inertia, allow system survival, and prevent adverse control interactions [8]. The authors of [9] reflect the technology readiness level of GFM converters and forecast the need for GFM converters in weak grid areas starting in three years

and in bulk grids within the next 10–30 years. Based on [8] the Grid Connection European Stakeholder Committee published a report [10] including a contribution how to integrate grid-forming into upcoming European Grid Connection Network Codes (GC NC). In [11] the EU Agency for the Cooperation of Energy Regulators (ACER) integrates these contributions into its proposal to amend the existing European GC NCs.

Due to the rapidly advancing transformation of power systems, experience with testing GFM in real grid situations is becoming increasingly important. The grid behavior of 23 wind turbines equipped with GFM control was investigated in the Scottish power system [12]. However, such field tests of GFM are rare due to the expense involved and limitations imposed by existing grid connection guidelines. There are few reports of laboratory-based testing of GFM converters on a large scale. For example, [13] presents fault ride through test results for GFM converters, showing how compatibility of GFM converters with existing grid code requirements can be achieved. However, the interaction of GFM converters at a power system level is usually studied using simulative approaches and often validated with hardware-in-the-loop simulations [14–16]. This paper presents, among others, lab-based testing of GFM converters on a megawatt-scale that demonstrates the grid stabilizing behavior of GFM converters from an interconnected system perspective.

The paper is structured as follows: Section 2 discusses the fundamental requirements for GFM converters from an interconnected grid perspective. Section 3 gives a survey and comparison of different known concepts for GFM control regarding their transient and stationary behavior. Section 4 introduces a test method for black box testing of GFM converters. Section 5 provides insight into testing activities that were performed to evaluate GFM converter behavior in various grid scenarios at a megawatt scale. Results from both a laboratory and field test campaign are presented. Section 6 addresses system aspects and stability studies. This includes, on the one hand, an approach to model complexity-reduced distribution network equivalents containing GFM converters in Section 6.1. On the other hand, Section 6.2 discusses the influence of different shares of GFL, GFM and SM-based generation on power system stability by analyzing system-split disturbances which induce a very high imbalance and Rate of Change of Frequency (RoCoF). The paper concludes with a summary and outlook in Section 7.

2 | FUNDAMENTAL REQUIREMENTS FOR GFM CONVERTERS FROM AN INTERCONNECTED GRID PERSPECTIVE

This section focuses on a high-level overview on GFM requirements from a grid perspective. Details on possible GFM implementations are provided in Section 3. Section 6 discusses details on the effect on the electric power system.

While several GFM concepts have been successfully applied in the context of microgrids, their application in large, interconnected power systems requires:

- detailed specification of the technical conditions under which a converter is considered to be GFM,
- specification of the behavior of GFM converters under emergency conditions (e.g. over-current limitation) and related boundary conditions for dimensioning GFM converters,
- evaluation of the system needs, that is, how much inertia and short circuit current are needed,
- quantitative and verifiable criteria that express the GFM contribution (e.g. inertia time constant).

In general, GFM converters have to fulfill the following fundamental requirements: In the first instant, they have to act as a stiff AC voltage source behind an impedance. Following this first instant, the angle, frequency and amplitude of the fundamental component of that voltage are allowed to change, but with a defined dynamic response. The requirements related to this transition phase between the instantaneous response and the steady-state behavior have to be well defined based on RMS-values, both with respect to active and reactive power. The internal voltage's frequency behavior following an active power imbalance has to be proportional to this active power imbalance.

Similar as for SM, this property has the consequence that GFM converters provide an instantaneous—neglecting electromagnetic transients—reaction of their current (and subsequently of active and reactive power) following any event in the power system, such as voltage faults, phase angle jumps or active power imbalances.

However, unlike SM, converters are not capable of providing currents significantly beyond nominal current. It is currently discussed whether grid-forming converters should provide an over current capability or not. However, the authors consider this not an issue for the individual converter as assessed in Section 4, but an issue that needs to be solved on the level of the power system, for example, by increasing the share of grid-forming converters as discussed in Section 6. Hence, GFM converters have to control their internal voltage in such a way that the power electronics are protected from harmful overcurrents. While limiting currents, the contribution of GFM converters to the fundamental requirements mentioned above is reduced. This is because the converters are not able to follow the equations of the applied control model. Instead, they have to limit their currents to the maximum capable. Due to this nonlinearity, the synchronizing "torque" may become insufficient and system stability may be at risk [17, 18]. Therefore, it is vital that GFM control includes mechanisms to maintain both synchronism and a sinusoidal internal voltage form while current limitation is active.

Furthermore, this behavior must be implemented such that it supports small signal stability of the system [19]. While the power of a single unit may be small, a large number of such units have a relevant impact on overall power system stability, as will be the case if a large share of the generation behaves in a similar way. The impact of a GFM converter on power system stability can be evaluated in a simplified way by considering GFM converters in island operation, that is, supplying only a single load. In order to contribute to system stability, GFM converters must operate stably under such conditions.

It is the responsibility of transmission system operators (TSO) to identify the system needs for GFM devices. Within the interconnected power system of continental Europe, system splits were identified as the determining contingency for the need for inertia. In [20], ENTSO-E identified the need for inertia in the interconnection of Continental Europe based on a study on possible system splits. In [21] and [22], the needs regarding fault level for specific grids have been evaluated.

3 | SURVEY AND COMPARISON OF GFM CONTROL CONCEPTS

From a grid perspective, the behavior of conventional GFL converters is characterized by fast current control. The corresponding setpoints of the currents are controlled based on deviations of active and reactive power from their respective setpoints. In addition to the described control cascades, grid synchronization by means of a phase-locked loop (PLL) is also crucial for the transient behavior of GFL converters. Grid synchronization of SM, which can be considered as the GFM textbook example, is based solely on power deviations. Together with the inertia of the SM and the effective internal voltage, the resulting behavior is a consequence of its physical properties. In contrast, the dynamic behavior of a GFM converter only depends on its GFM control concept, opening a wide range of possible implementations.

The variety of GFM control concepts developed so far shows that the general understanding of the synchronization behavior of GFM converters is very similar, that is, that it is based on the same fundamental principle of power synchronization as SM. The GFM control concepts generally generate setpoints for phase angle θ and amplitude $\hat{u}$ of the internal voltage to be set by the converter based on active and reactive power deviations. Usually, a distinction is made between an active power-frequency part and a structurally very similar reactive power-voltage part. This approach relies on the assumption of decoupled underlying mechanisms, that is, the ability to control active and reactive power separately. This assumption is justified in networks with a high X/R-ratio, as in extra-high and high-voltage grids. In case of grids with a low X/R-ratio, the two parts interfere with each other so that additional measures might be needed [23]. Despite this similarity among different GFM concepts, there are differences with respect to their transient behavior and how exactly synchronization with the grid is achieved.

Most commonly discussed GFM control schemes available in the literature are composed, with a few exceptions, of linear time-invariant transfer functions. The largest groups are virtual synchronous machines and droop-based synchronization methods. The former deduces their dynamic behavior from the SM, which they replicate in a simplified manner [24]. A typical example of this group is the Virtual Synchronous Machine 2nd order (VSM), which is based on the well-known second order swing equation. Droop-based concepts utilize a frequency-power droop with a time behavior characterized by introduced, but optional, lags. Typical representatives of droop-based concepts are the control concept simply known as Droop [25], its extension *Selfsync* [26], or the Power Synchronization Loop (PSL) [27], which, in contrast to the former, does not introduce an additional lag between the power input and the converter frequency. Another important example is the Voltage Control Mode Inverter (VCI) [28], which has a PI system between the active power input and the converter frequency. There are several extensions to the control concepts mentioned, which are intended to improve certain properties of the control concepts, such as preventing the provision of Frequency Containment Reserve (FCR, also known as primary reserve) in case of permanent frequency deviations, or the damping behavior [29].

The comparison of the above-mentioned control concepts on the basis of their block diagrams is usually difficult. Possible similarities and differences in their dynamic behavior are hard to identify. Converting the control concepts into their basic mathematical form in terms of transfer functions, however, allows for a straightforward comparison and enables further analyses on their dynamic behavior largely independent of a specific parameterization. The basis of this procedure is that the control concepts mentioned can be transformed into a single-input-single-output (SISO) transfer function

$$G_{p\theta}(s) = \frac{\Delta\theta(s)}{\Delta p(s)}, \tag{1}$$

between the active power input $\Delta p(s)$ and the phase angle output $\Delta\theta(s)$. Based on the linear time-invariant transfer functions of the control concepts mentioned above and compiled in [29], which can be transformed into a polynomial representation, the general transfer function

$$G_{p\theta}(s) = \frac{B(s)}{A(s)} = \frac{\sum_{j=m}^{M} s^j b_j}{\sum_{i=n}^{N} s^i a_i}, \tag{2}$$

can be identified. This general transfer function can represent these control concepts by selecting the respective parameters a_i and b_j of the denominator polynomial $A(s)$ with degree N and the nominator polynomial $B(s)$ with degree M, respectively. The control concepts mentioned in the literature have maximum numerator degree of $M = 2$ and maximum denominator degree of $N = 3$.

The dynamic behavior of the control concepts is based on the choice of parameters and is hard to compare by means of simulations. Analogous to [29], however, a straightforward comparison based on the instantaneous and stationary behavior can be carried out for a stepwise change in $\Delta p(t)$, assuming that Δp is small enough so that nonlinear limits are not reached. Here, the focus is on the acceleration behavior of the phase angle of the inner voltage of the converter $\ddot{\theta}(t)$. The acceleration behavior of the converter phase angle in the frequency domain,

$$\ddot{\theta}(s) = s^2 G_{p\theta}(s) \Delta p(s), \tag{3}$$

is derived by differentiating twice in time domain, which corresponds to multiplying the general transfer function given in (2) by s^2. Subsequently, the reciprocal values are calculated for two cases according to the final value theorem. In the first case, the behavior at the beginning of a stepwise excitation of Δp is calculated according to

$$\ddot{\theta}_0 = \lim_{t\to 0} \ddot{\theta}(t) = \lim_{s\to\infty} s\cdot\ddot{\theta}(s) = \lim_{s\to\infty} s\cdot s^2 G_{p\theta}(s)\cdot\frac{1}{s} = \lim_{s\to\infty} s^2 G_{p\theta}(s). \tag{4}$$

In this study, this relationship is interpreted as the instantaneous behavior of a control concept. Analogously, in the second case, the stationary behavior is analyzed according to

$$\ddot{\theta}_\infty = \lim_{t\to\infty} \ddot{\theta}(t) = \lim_{s\to 0} s\cdot\ddot{\theta}(s) = \lim_{s\to 0} s^2 G_{p\theta}(s). \tag{5}$$

Considering the reciprocals of the determined final values θ_0 and θ_∞ allows a straightforward characterization of the frequency response immediately and stationary after a stepwise change in $\Delta p(t)$. If the reciprocal of the instantaneous behavior $1/\ddot{\theta}_0$ tends towards zero, the frequency can perform stepwise changes. If, on the other hand, it tends towards a finite value, the instantaneous behavior of the GFM control concept is comparable to that of a SM. The instantaneous as well as the stationary behavior of the SM are characterized solely by its inertia time constant T_a. If, analogously, the reciprocal of the stationary behavior $1/\ddot{\theta}_\infty$ takes a finite value, then the stationary behavior of the GFM control concept is comparable to that of a SM. Note that we consider the SM without governor, which may modify the mechanical power driving the SM.

In case of $1/\ddot{\theta}_\infty \to \infty$, the GFM control concept provides permanent active power reserve for permanent frequency deviations, equivalent to FCR. In order to efficiently estimate the instantaneous and stationary behavior of a given grid-forming control concept based on its linear time-invariant transfer function, the relative degree

$$R = N - M, \tag{6}$$

can be utilized. GFM control concepts must always have a relative degree greater than or equal to 1. Otherwise, a feed-through would exist between the input and output, that is, between the active power and the converter phase angle. This would contradict the basic paradigm that GFM corresponds to an effective internal voltage phasor incapable of performing stepwise changes. In addition to the relative degree, in this study, we consider the number of poles equal to 0, which is referred to as the inherent integration S [30] of the GFM control concept. The inherent integration S is used as a benchmark for the integral behavior of a given control concept. Based on the linear control concepts in the literature with a maximum denominator degree of $N = 3$ and $R \geq 1$, $R, S \in \{1, 2\}$ must be considered. These four categories differ in terms of their instantaneous and stationary behavior. For relative degree $R = 1$ the converter frequency of the GFM control concept can perform stepwise changes, while for $R = 2$ the instantaneous behavior is comparable to that of a SM. For the case $S = 1$, the GFM control concept is characterized by a provision of FCR in the event of a permanent frequency deviation, while for $S = 2$ a finite stationary behavior analogous to the provision of inertia of SM is given. For $R = S = 2$, both instantaneous and stationary behavior of the GFM control concept are comparable to that of SM.

The presented methodology is performed for selected GFM control concepts. Related block diagrams and additional information on the GFM control concepts below are given in [29]. As the first control concept, the VSM 2nd order is represented by the transfer function

$$G_{p\theta,\mathrm{VSM}}(s) = \frac{1}{s}\frac{1}{sT_a + k_d}. \tag{7}$$

The transfer function of the VSM represents the inertial behavior of a virtual flywheel with the inertia constant $2H = T_a$, analogous to the modeling of the behavior of SM by the well-known swing-equation. The damping of the SM is introduced by means of the damping factor k_d. The transfer function of the VSM is equivalent to that of the Droop [25], given by the transfer function

$$G_{p\theta,\mathrm{Droop}}(s) = \frac{m_p}{s}\frac{1}{sT_\omega + 1}. \tag{8}$$

Due to $R = 2$, the frequency responses of VSM and Droop are both comparable to the response of the SM, but due to $S = 1$, FCR is provided. To mitigate the FCR provision, the VSM can be extended by an autonomous frequency (AF) tracking according to

$$G_{\mathrm{AF}}(s) = \frac{\omega(s)}{\Delta\omega(s)} = \frac{sT_{\mathrm{AF}} + 1}{sT_{\mathrm{AF}}}, \tag{9}$$

which adjusts the operating point of the frequency [29]. A block diagram of the resulting GFM control concept adapted for the purposes of this paper is given in Figure 3. The resulting transfer function of the VSM with autonomous frequency (VSMAF) is given by

$$G_{p\theta,\mathrm{VSMAF}}(s) = G_{p\theta,\mathrm{VSM}}(s)\,G_{\mathrm{AF}}(s) = \frac{1}{s^2 T_{\mathrm{AF}}}\frac{sT_{\mathrm{AF}} + 1}{sT_a + k_d}, \tag{10}$$

which results in $S = R = 2$ and thus leads to a behavior comparable to that of a SM. The control concept *Selfsync*, as an extension of the Droop given in (8), is given by the transfer function

$$G_{p\theta,\mathit{Selfsync}}(s) = \frac{m_p}{s}\frac{sm_{pp} + 1}{sT_\omega + 1}. \tag{11}$$

Due to $R = S = 1$, the control concept loses instantaneous behavior known from SM. A conclusion analogous to *Selfsync*

TABLE 1 GFM Control Concepts and evaluation of their instantaneous and stationary behavior based on the relative degree $\boldsymbol{R}$ and inherent integration $\boldsymbol{S}$.

Control concept	R	S	Instantaneous behavior $1/\ddot{\theta}_0$	Stationary behavior $1/\ddot{\theta}_\infty$
VSM	2	1	T_a	∞
Droop	2	1	T_ω/m_p	∞
VSMAF	2	2	T_a	$k_\mathrm{d}\,T_\mathrm{AF}$
Selfsync	1	1	0	∞
PSL	1	1	0	∞
VSM0H	1	1	0	∞
VCI	1	2	0	$1/K_{\omega\mathrm{i}}$
SM $G_\mathrm{SM}(s) \approx \frac{1}{s^2 T_a}$	2	2	T_a	T_a

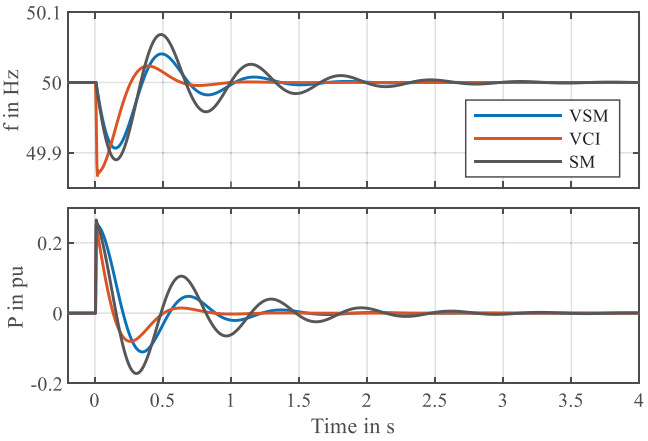

FIGURE 1 Simulation results of selected GFM control concepts in case of a phase angle jump to show the difference in their instantaneous behavior. The frequencies shown are the internal frequencies of the control concept to be provided by the converter.

can be derived based on the transfer function of the PSL

$$G_{p\theta,\mathrm{PSL}}(s) = \frac{k_p}{s}, \tag{12}$$

and the Virtual Synchronous Machine Zero Inertia (VSM0H) [31]

$$G_{p\theta,\mathrm{VSM0H}}(s) = \frac{D_\omega}{s}\,\frac{s\,(\tau_\mathrm{kD} + k_\mathrm{D}) + 1}{s\tau_\mathrm{kD} + 1}. \tag{13}$$

The control concept VCI, given by its transfer function

$$G_{p\theta,\mathrm{VCI}}(s) = \frac{sK_{\omega\mathrm{p}} + K_{\omega\mathrm{i}}}{s^2}, \tag{14}$$

has a frequency behavior capable of performing stepwise changes due to $R = 1$, but the stationary behavior of the VCI is again comparable to that of a SM due to $S = 2$. An overview for the analysis of the instantaneous and stationary behavior of the GFM control concepts is given in Table 1. The simplified model of the dynamics of the SM is used as a benchmark for instantaneous and stationary behavior. This simplified frequency behavior can be characterized by a double integrator. This corresponds to the widely used approach of modeling the mechanical part of the SM for interconnected power system studies. Within this approach, the damping components of the SM are included in Δp.

Whereas stationary behavior is used to characterize the ability of the control concepts to provide FCR and is thus easily understood, the instantaneous behavior is generally a more complicated relationship to envision. For this reason, two selected control concepts with distinct instantaneous behavior are compared in Figure 1 with the behavior of the SM in the case of a phase angle jump. The phase angle jump causes an almost stepwise change of the internal frequency in Figure 1 (top) for the control concept of the VCI, while only an at first ramp-shaped change in frequency can be observed for the VSM. A similar frequency behavior can be observed for the SM due to its modeling based on its physical properties. However, it can also be observed that the instantaneous active power output in Figure 1 (bottom), being due to the phase angle jump, is identical in all three cases. Differences in the subsequent transient behavior are parameter-dependent only.

4 | PROCEDURE FOR TESTING GFM CONVERTER PROPERTIES

As it can be seen in the previous section, different implementation methods are leading to different characteristics. Therefore, an essential step to validate GFM converters is to agree on an exact definition and specification of their electrical behavior as well as to define a suitable conformity assessment procedure that enables this in a black box approach, without any insight in the implementation of the control software. For converters that can be tested in a laboratory, a standardized testing guideline for GFM converters is needed to evaluate the relevant requirements. In [32–34], and [35], such a procedure is proposed.

In addition to the fundamental requirements described in Section 2, the testing guideline suggests clustering the testing of GFM into four groups as illustrated in Figure 2: voltage source properties, power quality, inertial response, and overload behavior.

The test for the voltage source property determines the dynamics of the voltage control as well as the internal impedance. This is done by suddenly islanding the GFM converter together with a load that is adjusted to different active and reactive power settings. Prior to the islanding the converter is operated in parallel with the load on grid at a power setpoint of zero. At the moment of disconnection from the grid, the converter needs to take over the load and stabilize the voltage. To characterize the dynamics of the voltage source, the voltage

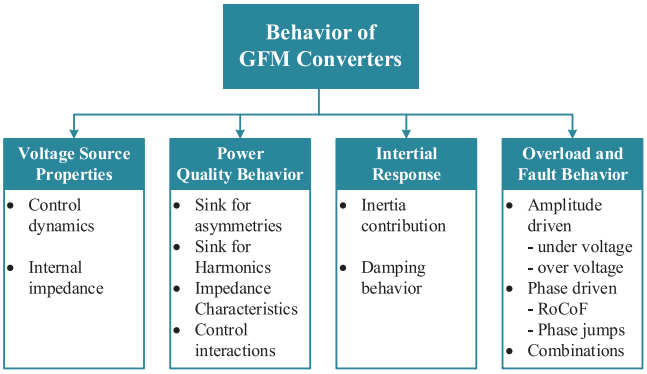

FIGURE 2 Structure of the procedure for the testing of GFM converters.

reaction time t_{VR} as well as the internal impedance $\underline{Z}_{GFC,int}$ are evaluated according to the described procedure in [33].

To demonstrate power quality behavior, the GFM converter needs to act as sink for harmonic and asymmetric voltages and therefore improve the power quality at its point of connection. Thus, in case of an asymmetric voltage, it must be verified that the GFM converter provides a current counteracting these asymmetries. To characterize this behavior, we consider the reduction of the unbalance factor Δa_{unb} when connecting a GFM converter to a grid that is distorted by a defined asymmetric load. Regarding its behavior to improve the harmonic content of the grid voltage, the reduction of the total harmonic distortion ΔTHD_u of the grid voltage, distorted by a defined non-linear load, when connecting a GFM converter, is evaluated. In addition, it must be tested within which frequency range the converter can provide harmonic currents to counteract harmonic voltage distortions. To characterize this, the harmonic current exchanged with the grid is evaluated. This is done by calculating the exchange factor $a_{exch,h}$ representing the sum of the harmonic current from the grid and the GFM converter divided by the harmonic current of the load. As long as this factor is at around one, no significant harmonic current is exchanged with the grid. A value significantly above one, on the other hand, indicates the contrary, raising the need for further analysis of the results. To analyze potential interactions of the GFM converter with the grid in more detail, the frequency-depending characteristic of the internal impedance $\underline{Z}_{GFC}(f)$ as well as the internal voltage source $\underline{V}_{GFC,i}(f)$ is evaluated using the method of the differential impedance spectroscopy [33].

As the first two properties are primarily related to the instantaneous behavior of the voltage source, the inertial response focuses on the defined limited dynamic response of the internal voltage amplitude and angle. Thus, the ability of a GFM converter to provide inertial response and damping. As the GFM converter behavior does not rely on physical properties there is a possibility that inertial response as well as the damping behavior can differ from that of a SM and also regarding different grid events as shown in the previous section (e.g. phase jumps, frequency changes). Therefore, multiple tests must be carried out, like a voltage phase jump or a frequency ramp. At these tests, the inertia constant H and the damping characteristic represented by the coefficient D, which represents the envelope of a damped oscillation, are evaluated. For more details, see [34].

The last part of the testing guideline deals with behavior of the GFM converter during severe grid events. As described in Section 2, such events may lead to reduction or the loss of grid-forming behavior and, thus, to stability problems. Therefore, the converter must demonstrate its grid stabilizing behavior and stable operation also during such events. Here, four different types of events as well as combinations are evaluated: over, under voltage and phase jump events as well as fast frequency changes. The evaluated requirements for voltages faults (over and under voltage) are the injection of a voltage supporting fault current with an immediate reaction corresponding to the electromagnetic time constants in the power systems, typically within a few milliseconds. For example, [8] suggests a desired reaction time of less than 5 ms. Furthermore, there are requirements regarding stable operation (no desynchronization, no oscillations) and return to pre-fault condition directly after the fault with a similar reaction time as at beginning of the fault. For phase jump events, an instantaneous injection of nominal active power to counteract the phase angel change is required. To this end, the time $t_{0.9}$ needed to reach 90% of the required power is measured. Moreover, the GFM converter needs to return to pre-fault conditions directly after the event. In order to characterize this, the times $t_{P_{set}}$ and $t_{Q_{set}}$ needed to reach the active and reactive power setpoints, respectively, are measured. In case of a fast frequency change, the main requirement is to inject the nominal active power to counteract the frequency change. After the frequency change, the GFM converter should return directly to its pre-fault settings, which is why $t_{P_{set}}$, $t_{Q_{set}}$ are measured also for this event. Of course, tripping of the converter should not occur at any event. Moreover, stable operation is necessary. Hence, neither desynchronization nor high oscillations are acceptable. In case of combined faults, the same requirements are evaluated as for single events. Moreover, the reaction on the second event is of importance as it shows that the GFM retains its voltages source properties despite the first event [35].

5 | GFM CONVERTER TESTING

In this section, the behavior of GFM converters is investigated in a laboratory test campaign. The objective is to test the behavior of developed GFM converters by applying the criteria of Section 2 and to validate it with the test methods of Section 4 in parallel operation, current limitation, and its impact on the stability of the interconnected power system.

The developed GFM converter uses the VSMAF as control scheme, implemented on a 50 kVA battery converter with a commercially available hardware. Figure 3 depicts the block diagram of the according control concept, which is based on a VSM control that has been enhanced with an additional feedback (autonomous frequency). As a result, the VSMAF control, like a SG, contributes to inertia but does not provide FCR (Frequency Containment Reserve). A more detailed description of the control concept can be found in [29], referred to as "Swing Equation with Autonomous Frequencies (SEAF)". However,

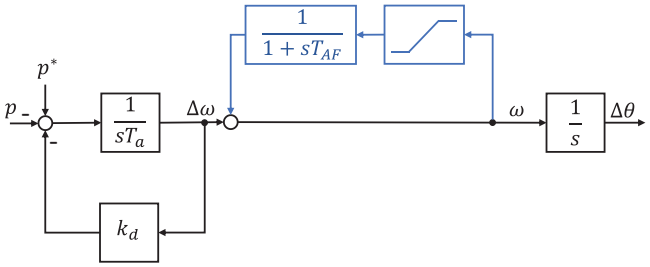

FIGURE 3 Block diagram of the extended VSMAF with a limiter in the frequency feedback (marked in blue).

in the case of critical grid conditions, it may be necessary to additionally provide $P(f)$ and $Q(U)$ control functions. For this reason, the control has been extended to act like a VSM outside of adjustable frequency and voltage limits. This was achieved by the implementation of limiters for the autonomous frequency, as indicated in Figure 3, and for the voltage feedback. As both VSMAF and VSM have some drawbacks regarding the current limitation, additional functional features were added that prevent possible loss of grid synchronism even during severe grid faults and maintain the voltage source behavior in such cases. Those additional functional features are not described in detail due to intellectual property reasons. They are, however, similar to the method described in [29].

For the overall measurement campaign, a total of twelve converters with a summed nominal power of 600 kVA are available, each of which can be operated with a GFL or GFM control. In addition, a load-bank and synchronous generator (SG) are in use. All sources and loads are connected to a medium voltage busbar via a transformer. With the help of impedances on the medium voltage line, an interconnected system with two nodes could be realized. The given test setup allows to test for example active and reactive load changes, over- and under-voltage-ride-through (OVRT/UVRT), phase jump and system split events. In the following, selected results are presented to describe the observed behavior of the GFM converters in more detail.

5.1 | UVRT-tests

This test analyses and compares the behavior of the GFM converter in normal operation and in critical grid condition in two UVRT cases. In this case, the critical grid condition is defined at a voltage deviation such that the voltage falls below 90% of its nominal value. It should be noted that the selected critical condition does not represent the worst-case scenario from the system perspective, as there is still sufficient margin to the maximum power. However, from the converter's point of view, the current limit is reached in the given situation, which corresponds to the worst-case scenario from a converter perspective. For this test, the voltage limits of the additional feedback path (Figure 3) were set to ±10% around the nominal voltage. As explained earlier, the response of the converter to the 95% UVRT should correspond to the VSMAF, while the 75% UVRT align with the VSM behavior.

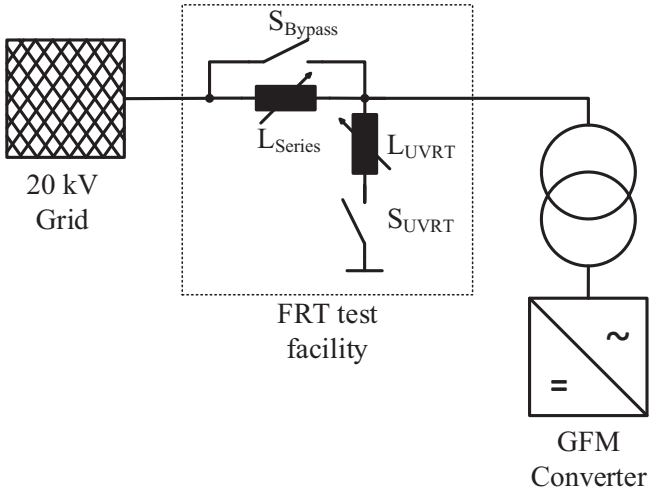

FIGURE 4 Laboratory setup for the UVRT test according to IEC 61400-21-1:2019.

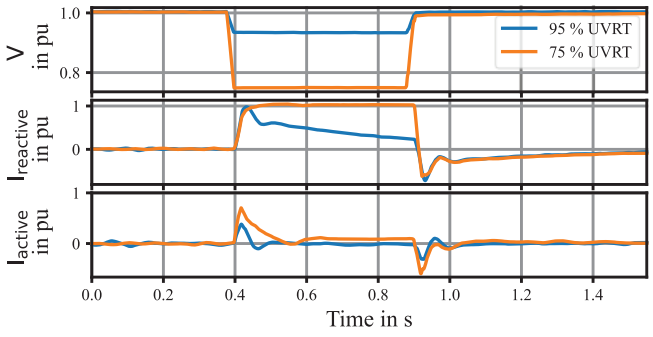

FIGURE 5 Active and reactive current for an 95% and 75% UVRT.

The test setup is shown in Figure 4. The GFM converter is connected to an FRT test facility via a transformer. This, in turn, is connected to the grid. The voltage drops are induced by using an inductive voltage divider. The test facility is activated by opening of $S_{Bypass.}$ At the moment of closing the event switch S_{UVRT} the voltage at the connection point of the GFM converter collapses according to the ratio of L_{Series} and L_{UVRT}. Due to the design of the FRT facility, a phase jump is generated in addition to the voltage drop.

The measurement results are given in Figure 5, showing the reactive and active currents. In both UVRT cases, the GFM converter reacts instantaneously, injecting reactive and active current. Thus, it acts as a voltage source to the voltage drop and the phase jump. Subsequently, the reactions differ. In the 95% UVRT test case, the GFM converter reacts as expected by returning to the reactive and active power setpoints, as it is still in normal operation. In the 75% UVRT test, however, the system voltage is outside of the normal range and the GFM converter injects its maximum reactive current, acting like a VSM. After the fault clearance, the converter injects voltage-lowering reactive current in both cases, as the internal voltage reference is lower than the pre-fault voltage due to the internal voltage feedback.

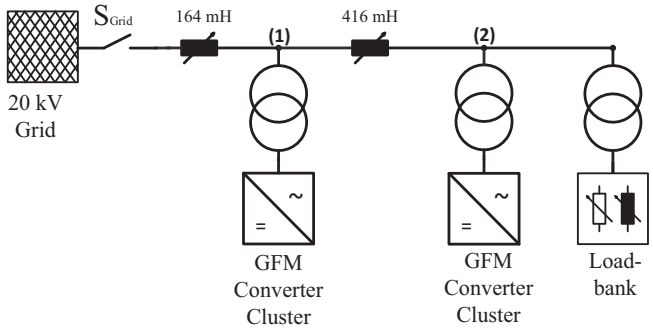

FIGURE 6 Simplified representation of the lab setup for the islanding test.

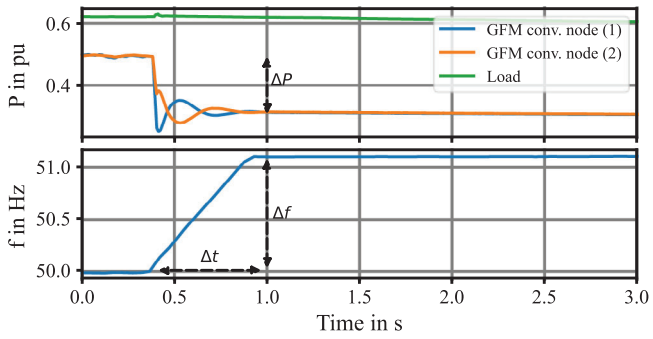

FIGURE 7 Active power response and frequency for the islanding test.

5.2 | Islanding test

The next test case addresses the islanding behavior of two GFM converters. This allows the analysis of the contribution to system inertia, the transition from normal operation (VSMAF) to the critical control (VSM) and load sharing. It may also provide evidence of small signal stability as mentioned in Section 2, since it proves the stability of control in a situation, where there is direct feedback between the inverter behavior and the grid, as emphasized in the ACPPM report [10]. The limits of the feedback frequency of the VSMAF for this test are set to 49 and 51 Hz.

The test setup is shown in Figure 6. At node (2), a load-bank and a GFM converter are connected. At node (1), which is separated from node (2) by an impedance, another GFM converter is connected. By opening the switch S_{grid}, the laboratory setup falls into island operation. Both converters are parameterized identically.

The measurement results are given in Figure 7. At the initial state, the total power generation of the GFM converters is 1 pu (each converter 0.5 pu), with the load having an active power consumption of 0.62 pu. Thus, the converters export 0.38 pu active power to the grid. At around 0.4 s, the switch S_{grid} is opened and the setup falls into island operation. A test case with power import is also possible, considering that in order to reach a stable island, the power available within the island must be sufficient to meet the power demand of the connected loads. As a result, the GFM converters reduce their active power depending on their respective proximity to the opening circuit breaker S_{Grid}, leading to a frequency increase up to around 51.1 Hz over 0.5 s. This test result perfectly shows the small signal stability mentioned in Section 2. Based on the frequency curve and the active power difference between the set points of the converters and the actual active power output, the inertia time constant of the island can be estimated by using the Equation (15).

$$H = \frac{P_N \cdot f_N}{2 \cdot \Delta P_{sum} \cdot \frac{\Delta f}{\Delta t}}. \tag{15}$$

The ΔP shown in Figure 7 is given for each converter, hence it must be multiplied by two for Equation (15). Inserting the corresponding values, the system inertia can be estimated to around 28 s. Changing the parametrization of the power controller, the system inertia can be adjusted to the desired value. In addition to the system inertia, the VSM behavior and load distribution is clearly visible. Up to the VSMAF feedback limit of 51 Hz only the inertia is effective resulting in a constant RoCoF. Above 51 Hz, the gain of the VSM becomes effective resulting in a continuous active power provision, which is equal in both converters, as the parametrization is identical. Since the VSM gain is only proportional, the frequency remains slightly above 51 Hz.

These measurement results of the UVRT and islanding test demonstrate that a GFM converter can be capable of supporting the grid in case of disturbances instantaneously and can support the grid in critical grid situations without actively switching the control mode. Furthermore, the VSMAF provides the required system inertia, with the VSM additionally enabling load sharing.

5.3 | Load step test

Next, a load step in grid-connected configuration is considered. Two test cases with different load heights will be analyzed. For the first test, the GFM converters remain within their current range, whereas, for the second test, the load is adjusted such that both converters reach their current limitation. Due to the chosen VSMAF control, the behavior should be similar to the SM as long as the nominal power is not exceeded. As soon as the current limitation is reached, the GFM converters should inject active power close to the nominal power and then return to their pre-event setpoint as the converter is grid connected and the load will be supplied by the grid. Furthermore, it can be investigated whether desynchronization occurs, meaning that the angle of the internal voltage phasor of the converter no longer synchronizes with the voltage phasor of the grid.

The test setup is depicted in Figure 8, which is similar to the previous one shown in Figure 6. The active power set point is set to zero and the control parametrization of the GFM converter is identical for both tests. The load step is induced by adjusting the value of the load bank to 100 kW for the normal operation and to 1000 kW for the current limitation scenario.

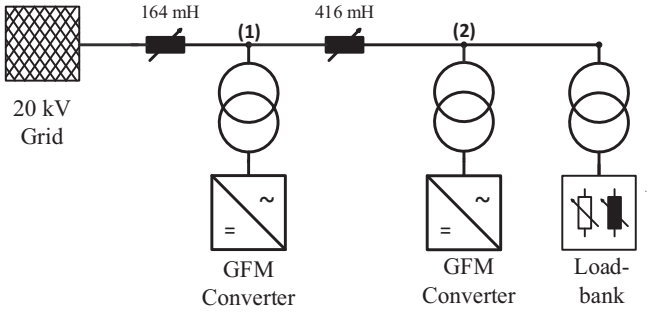

FIGURE 8 Test setup for the load steps.

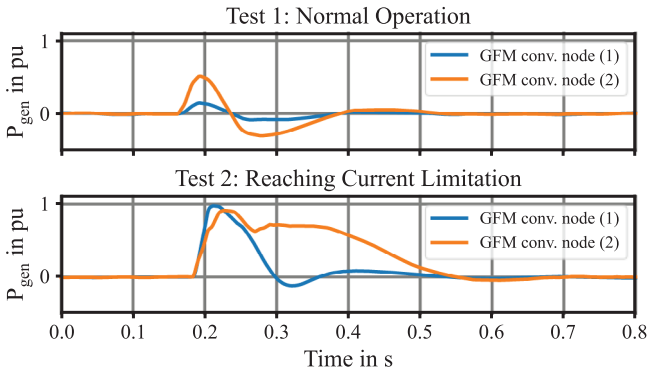

FIGURE 9 Active power responses for a load step in grid-connected configuration.

The results of the tests are shown in Figure 9. The upper plot displays the normal operation whereas the lower plot illustrates the current limitation case. All calculated values are based on an RMS calculation over one period of 0.02 s.

Looking at the upper plot, it is visible that both GFM converters react as a voltage source with an active power counteracting the load change depending on their respective proximity to the load bank. Subsequently, the active power is controlled back to the set point with a behavior similar to that of a synchronous machine.

Looking at the second test, both converters reach their current limitation after the load step. Due to the significantly lower proximity to the load at node (2), the current limiter of this converter must intervene more strongly than that of the converter at node (1). This stronger intervention is also reflected in the different settling behavior that follows. Given the severity of the fault, the converter at node (2) will require longer than the one at node (1) to return to its setpoint, with both cases providing well-damped behavior. In addition, the GFM converters remain stable and do not show any desynchronizing effects.

5.4 | Field test of GFM converters

After the GFM converters have proven their grid stabilizing capabilities during the test campaign, a field test in a real environment is carried out. For this purpose, four GFM converters are used to independently supply the office wing of Fraunhofer

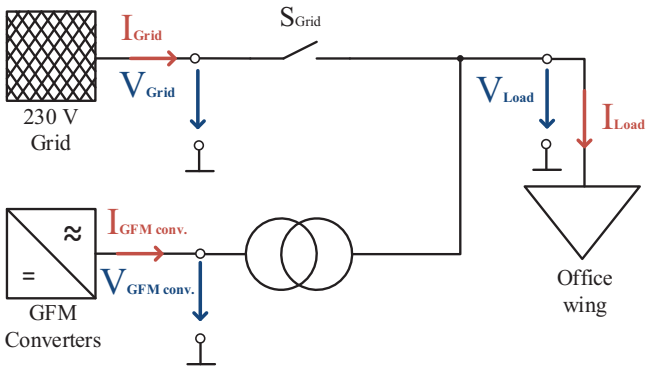

FIGURE 10 Test setup for the field test.

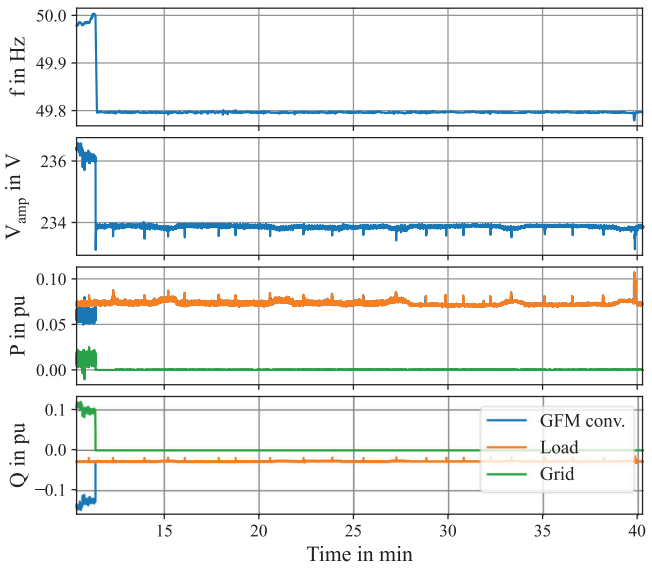

FIGURE 11 Measured voltage, frequency, active and active power during islanding.

ISE in Freiburg for about 1 h. The GFM converter cluster is connected to the office wing via a Dyn5 400/400 V transformer, shown in Figure 10. Using the switch S_{Grid}, the office wing can be disconnected from and connected to the public grid.

The parameterization of the GFM converters is slightly adjusted for the field test to ensure the best possible protection of the connected loads. The adjustment consisted of a reduction of the tolerance band for the voltage reference value to [227, 233] V and the frequency limits to [49.8, 50.2] Hz of the internal voltage source. In this way, the deviation of the voltage amplitude and the frequency of the island grid are limited to a narrow range around the nominal voltage of 230 V and frequency of 50 Hz. In order to obtain an adequate level of system inertia, the inertia parameter H of the converter control is set to 5 s. An overview of the first 40 min is given in Figure 11. Before the islanding at approximately five minutes, a reactive power exchange between the GFM converters and the grid is noticeable. This can be explained by considering the VSM behavior, as the voltage system voltage is outside of the tolerance band. It reacts due to the high grid voltage of 1.026 pu (236 V) and

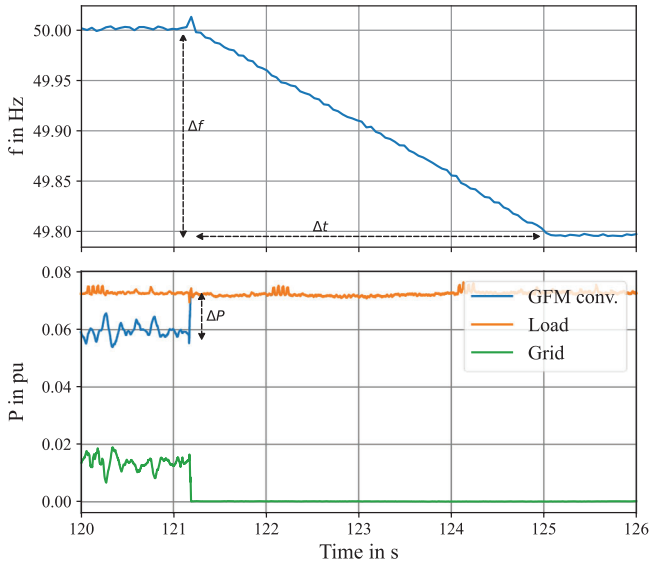

FIGURE 12 Measured frequency and active power during the disconnection to the public grid.

injects underexcited reactive power. After the islanding the frequency stabilizes at 49.8 Hz (0.996 pu) and the voltage at 233 V (1.017 pu). In the further course of the measurement, small power changes of the load can be seen again and again, resulting in a changing frequency and voltage. These load changes are supplied by the GFM converters without any issues.

Figure 12 shows the moment of the grid disconnection in more detail. Before islanding, the active power setpoints of the GFM converters are 0.02 pu below the load. Thus, the converters have to increase their power at islanding and the frequency decreases. By (15), the system inertia can be calculated to around 6.8 s, which is very close to the configured value, considering all neglected lags like the active power calculation.

6 | SYSTEM ASPECTS

So far, this paper mainly focused on the behavior of individual GFM converters. In this last section, we consider aspects of the analysis of system behavior. First, a method for aggregated and dynamically equivalent modelling of active distribution networks (ADN) with a high share of converter-based feed-ins is introduced. Subsequently, the influence of selected GFM control concepts on power system stability will be analyzed by means of interconnected power system simulations.

6.1 | GFM converter consideration in equivalent distribution network models

The increasing importance of dispersed generation in distribution systems necessitates a proper representation of these ADN in grid models for stability analysis. However, the distribution system generally is not of particular interest for such analysis. For this reason and because of a high computational effort and insufficient data availability, detailed ADN models may be substituted with equivalent dynamic ADN models (EDAM).

Stability analysis focuses on the transmission system in which the relevant faults occur. Therefore, the transmission system is modeled in detail. Previous work [36] elaborated the suitability of gray-box parameter identification methods for capturing the dynamic response of converter dominated networks in corresponding dynamic equivalents. However, with the introduction of GFM converters, new challenges arise for the derivation of EDAM [37].

The dynamic behavior of GFM converters is highly dependent on the grid strength at the GFM converter's point of common coupling (PCC) and the electrical distance to the fault location. Voltage sensitivities $\frac{\partial V_i}{\partial P_i}$, $\frac{\partial V_i}{\partial Q_i}$, $\frac{\partial \vartheta_i}{\partial P_i}$, and $\frac{\partial \vartheta_i}{\partial Q_i}$ at the PCC i of the GFM converter in the detailed network are a suitable measure for considering these factors in EDAM [38]. Also, the detailed network's topology in terms of GFM converter location needs to be considered in the EDAM to properly reproduce the GFM converter's dynamic behavior.

In [38], a method is proposed to derive EDAM from detailed ADN models containing GFM converters. The proposed approach is called Sensitivity-Technology-Control-Clustered Approach (STCA) and can be sketched as follows: First, the loads and GFL converters per voltage level of the detailed ADN model are clustered according to technology and control strategy. Each GFM converter in the detailed network is assigned to an individual cluster to optimally consider the GFM converter location within the detailed network in the EDAM.

In a second step, the equivalent transformer connecting the EDAM with the boundary bus is created. The boundary bus is defined as a common link between the transmission system and the ADN. The loads and GFL converters are aggregated according to the clusters and connected to the lower voltage side of the equivalent transformer. Active and reactive power demand and generation of each equivalent component is given by the sum of the active and reactive power demand and generation of each component in the respective cluster in the detailed ADN model. The equivalent GFM converters are connected to the lower voltage side of the transformer with an impedance according to the detailed network's topology. The parameters of these impedances are tuned to achieve the same voltage sensitivities at the PCC of the equivalent GFM converter compared to the same in the detailed ADN model. Moreover, an additional slack load is utilized so that the steady-state power flow at the boundary bus of the EDAM matches the one at the boundary bus of the detailed ADN model. An EDAM aggregated by STCA is shown exemplarily in Figure 13b.

The performance of the proposed method is illustrated by simulation results in the following. As a test network model, a 10 kV radial distribution network of the open-source tool DINGO [39] as shown in Figure 13a is used. The total load is 40 MW and 10 Mvar. 99% of the load is covered by converter-based generation and 60% is generated by six distributed GFM converters. The external grid is modeled as a voltage source connected to the distribution network with a transmission line of

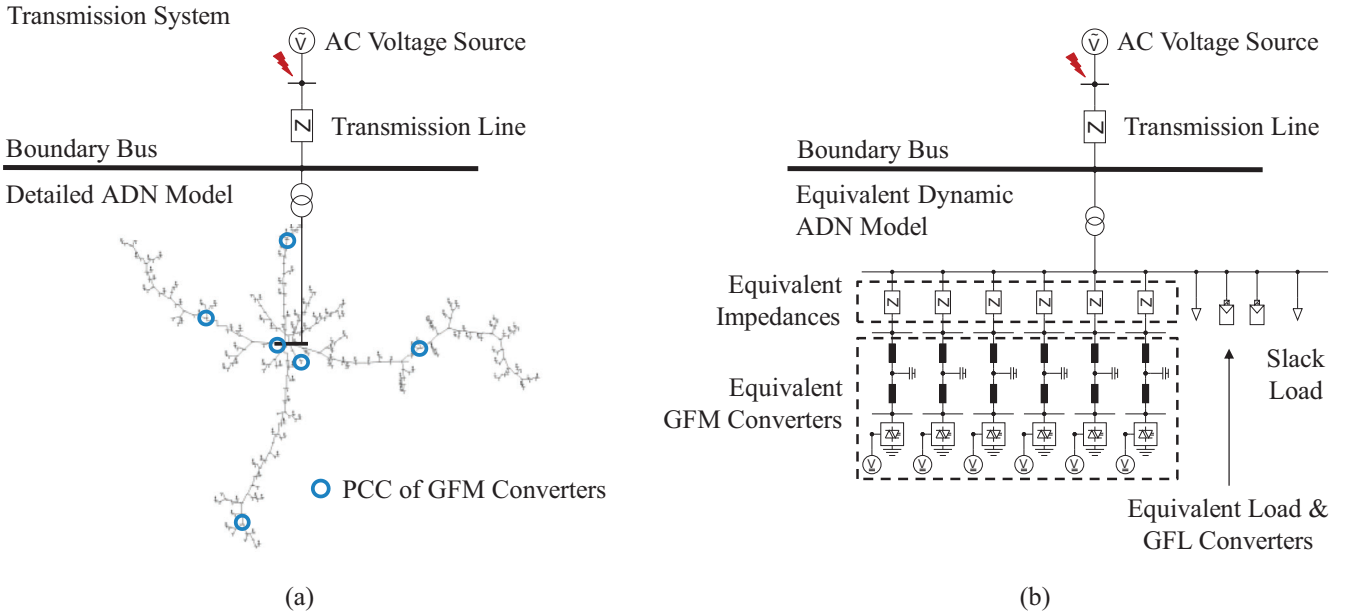

FIGURE 13 Schematic of detailed ADN model (a) and EDAM aggregated by STCA (b).

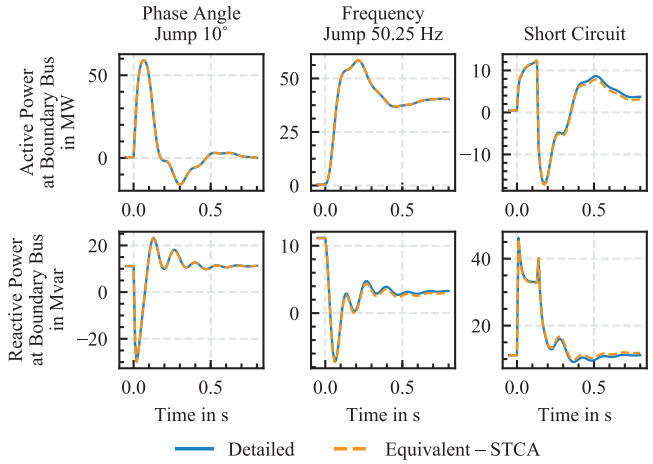

FIGURE 14 Active power and reactive power flow at boundary bus of detailed network model and EDAM; positive reactive power values: over-excited state; negative reactive power values: under-excited state.

50 km length. The EDAM aggregated by STCA is shown in Figure 13b. Since all GFM converters are located in separate branches in the detailed network model, the equivalent GFM converters are connected in parallel in the EDAM. Three events are investigated in the following: a phase angle jump from 0° to 10°, a frequency jump from 50 Hz to 50.25 Hz, and a 130 ms three-phase short circuit. Both phase angle jump and frequency jump events are induced by the voltage source. The short circuit is located at the PCC of the voltage source. All events occur at 0 s.

In Figure 14, the active and reactive power flows at the boundary buses of both the detailed network model and the EDAM are shown. As the figure shows, the responses of the EDAM are very close to those of the detailed model for all three events and for both the active and reactive power flows. The size of the detailed ADN model is reduced significantly from 195 nodes to only 7 nodes. Additionally, simulation time of the EDAM decreases by 97.3% compared to the detailed simulation. This exemplary simulation can be conducted for other network models, for example, with a higher number of GFM converters, with similar results. Hence, the proposed method appears to be very suitable to create EDAM capable of capturing the detailed network's dynamic behavior.

6.2 | Influence of GFM converters on power system stability

Even though GFM converters are controlled in such a way that they mimic essential properties of SM, they are fundamentally different from a hardware perspective. Instead of a voltage source that is based on the induction by a rotating magnetic field, the AC voltage is created by fast switching of power electronic devices at frequencies of several kHz, depending on the type of power electronics used and on the configuration of the converter. In order to analyze the behavior of single GFM converters, detailed models have been created that are able to reflect the real behavior of the GFM implementation on a converter hardware with a very high level of detail.

However, the complexity of such models prohibits their use in the context of power system dynamic stability studies. Hence, the question arises how GFM converters should be modeled in this context. Simplifications are required in order to obtain models that can be used as sub-models of large power system models. However, these simplifications need to be adequate in the sense that they should not have an impact on the conclusions of such a study.

Two common simplifications are (a) the use of an average value model (AVM), meaning that the output voltage is generated by means of a three-phase AC voltage source, possibly neglecting converter internal processes and controls and (b) the assumption that the DC voltage is constant, corresponding to the simplification that an infinite, or at least appropriately dimensioned, energy storage capacity is available for each GFM converter. Both are considered as reasonable assumptions in the context of power system stability studies.

A further simplification commonly used for such studies is the representation of voltages as phasors in a suitable rotating coordinate system (usually Park coordinates). This representation usually is denoted as "RMS". A key advantage of RMS-models is that the phasor variables (angle relative to the reference coordinate system and amplitude) change much slower than the physical values. Hence, the simulation of the model can be performed with larger time steps and, thus, significantly less computational effort. Phasor based modeling is justified if all system voltages are nearly sinusoidal, that is, for SM, GFL converters in strong grids and GFM converters that are operating in GFM mode.

However, this is not true for the case of GFM with active current limiting, as the voltage provided may not be sinusoidal anymore and is not represented adequately by a phasor. However, the effect of current limits on system stability may be significant, as shown in [17, 18]. The same is true for GFL converters in weak grids, where instability may arise from interactions between controls and grid voltage at frequencies other than the fundamental frequency. For this reason, EMT (electromagnetic transient) models, which do not represent voltages and currents as phasors but rather use their instantaneous physical values over time, of a power system of limited complexity were developed to validate simulation results obtained with RMS models and to further evaluate the effects of dynamics that are not adequately modeled in RMS simulations.

The EMT transmission system simulations of this section are performed using a benchmark network model of the transmission system of the German federal state of Baden-Württemberg and is shown in Figure 15. The simulations consider islanding of the benchmark network model while having an export surplus of 25%, which leads to a strong increase of system frequency. To show the difference in the instantaneous behavior of the control concepts on frequency stability (as demonstrated in Section 3), the VSMAF and the VCI are compared. The frequency of the VCI is able to perform stepwise changes, whereas the VSMAF is not. However, the control concepts are parameterized such that their stationary inertia contribution is identical after a finite time.

The maximum RoCoF that occurred among all nodes in the simulations for the VSMAF control concept are shown in Figure 16, whereas the simulation results for the VCI control concept are shown in Figure 17. The shares of SM, GFM and GFL have been varied in steps of 10%. Based on the maximum RoCoF, the minimum share of SM or GFM is derived by means of a maximum permissible RoCoF of 2 Hz/s. For this purpose, the RoCoF was determined over a moving 60 and 500 ms window. The results show that, unlike SM and GFM converters, GFL converters do not contribute to power system inertia. Therefore, higher shares of GFL converters with today's control concepts lead to higher RoCoF. In a direct comparison of the simulation results of the control concepts, it is noticeable that negative effects on the RoCoF caused by the instantaneous behavior of the control concepts become apparent especially with the shorter window length of 60 ms. When the VCI is

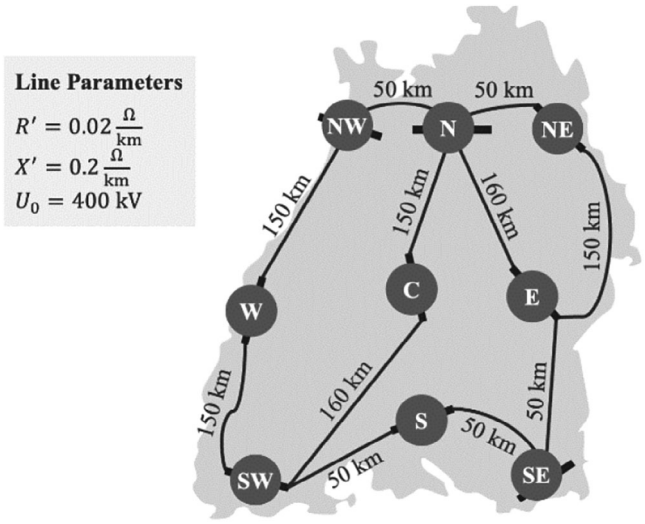

FIGURE 15 9-bus-network model of the transmission system simulations.

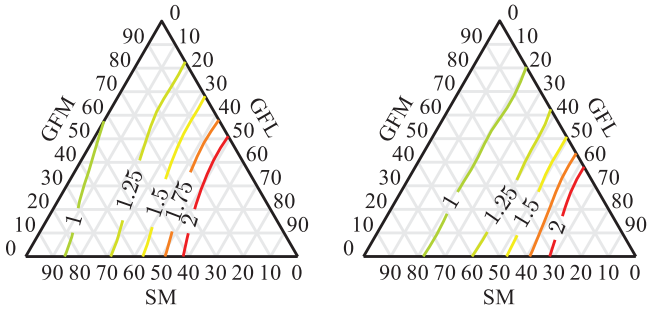

FIGURE 16 Ternary diagram with maximum RoCoF in Hz/s determined over a moving 60 ms (left) and 500 ms (right) window for different shares of SM, GFL and GFM with the VSMAF control concept after a 25% export loss.

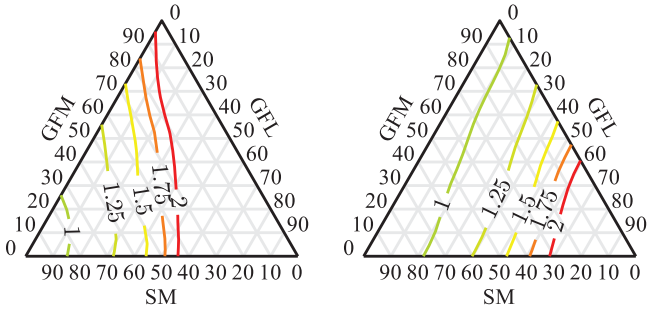

FIGURE 17 Ternary diagram with maximum RoCoF in Hz/s determined over a moving 60 (left) and 500 ms (right) window for different shares of SM, GFL and GFM with the VCI control concept after a 25% export loss.

applied, the critical threshold of 2 Hz/s is already exceeded at smaller shares of GFM compared to the VSMAF. These differences and the effect on exceeding the critical RoCoF threshold become less apparent when analyzing the situation over the longer window of 500 ms.

Depending on the specific grid situation, especially in the case of a weak grid connection of GFL converters, oscillatory instabilities may occur even with a higher proportion of GFM contributions. In addition, the simulation studies only considered situation with a surplus of available power (over-frequency events). The system issues relating to the operation of feed-ins close to or at their operating limits in the event of a lack of power (under-frequency event) require further comprehensive investigations.

7 | SUMMARY AND OUTLOOK

The use of GFM converters is vital to ensure stable interconnected power system operation with high converter penetration. Therefore, a GFM converter must first behave as an AC voltage source behind an impedance. The fundamental components of the internal voltage (amplitude, frequency, phase angle) are allowed to change, but with a defined dynamic response. It is crucial that the internal voltage's frequency behavior is proportional to this active power imbalance. The paper presented a method for characterizing the nature of the dynamic behavior of specific GFM control concepts. It can be shown that there are significant differences between most common GFM concepts in terms of their instantaneous and steady-state behavior. Future work needs to determine how critical concepts that have zero instantaneous inertia are to system stability. Laboratory tests at megawatt scale have shown that GFM converters with a suitable configuration can stabilize power systems in critical situations, such as system splits or phase jumps. Based on this experience, the specifications defined for GFM behavior have been translated into a black-box test approach. The test procedure presented enables compliance testing of GFM products and can serve as a reference for converter designers, helping to correctly design grid stabilizing control schemes. The developed method to create equivalent dynamic active distribution network models (EDAM) allows to consider the dynamic behavior of GFM converters in distribution network models while reducing the model complexity significantly. This will get increasingly important for grid stability studies in systems with a raising penetration of GFM converters. Finally, investigations of interconnected power systems show that GFM converters can replace SM. However, the type of control method influences the frequency behavior, especially in the short-term response. This indicates that a special focus must be put on the short-term behavior of GFM in the future.

AUTHOR CONTRIBUTIONS

Soenke Rogalla: Funding acquisition; investigation; supervision; writing—original draft; writing—review and editing. **Philipp Ernst**: Investigation; writing—original draft. **Hendrik Lens**: Funding acquisition; investigation; project administration; supervision; writing—review and editing. **Thomas Schaupp**: Funding acquisition; investigation; supervision; writing—original draft. **Christian Schöll**: Investigation; writing—review and editing. **Roland Singer**: Investigation; project administration; writing—original draft. **Jakob Ungerland**: Investigation; writing—original draft.

ACKNOWLEDGEMENTS

This paper mainly summarizes the key findings of the joint research project VerbundnetzStabil (stable interconnected system behavior with converter-based generation). The authors gratefully acknowledge the financial support for this project by the German Federal Ministry for Economic Affairs and Climate Action (FKZ 0350015A-D) [40]. The authors would also particularly like to thank the company Kaco new energy GmbH which provided the inverter platforms for the laboratory tests.

CONFLICT OF INTEREST STATEMENT

The authors declare that they have no conflicts of interest related to this work.

DATA AVAILABILITY STATEMENT

The data that support the findings of this study are available from the corresponding author upon reasonable request.

ORCID

Soenke Rogalla https://orcid.org/0009-0003-8447-670X
Philipp Ernst https://orcid.org/0009-0006-5796-0848
Hendrik Lens https://orcid.org/0000-0002-0208-4100
Thomas Schaupp https://orcid.org/0009-0006-6968-9661
Christian Schöll https://orcid.org/0009-0002-4077-4599
Roland Singer https://orcid.org/0009-0006-0220-990X
Jakob Ungerland https://orcid.org/0000-0002-1796-8101

REFERENCES

1. Kundur, P.: Power System Stability and Control, new ed. McGraw-Hill Education Ltd, New York (1994)
2. Meinhardt, M., Rothert, M., Engler, A.: New V/f-statics controlled battery inverter: Sunny Island®—the key component for AC-coupled hybrid systems and mini grids. https://publica.fraunhofer.de/handle/publica/344358 (2003). Accessed 21 Dec 2023
3. Engler, A.: Regelung von Batteriestromrichtern in modularen und erweiterbaren Inselnetzen. Dissertation, University of Kassel (2002)
4. Unruh, P., Nuschke, M., Strauß, P., Welck, F.: Overview on grid-forming inverter control methods. Energies 13(10), 10 (2020)
5. Milano, F., Dörfler, F., Hug, G., Hill, D.J., Verbič, G.: Foundations and challenges of low-inertia systems (invited paper). In: 2018 Power Systems Computation Conference (PSCC), pp. 1–25. IEEE, Piscataway (2018)
6. Shakerighadi, B., et al.: An overview of stability challenges for power-electronic-dominated power systems: The grid-forming approach. IET Gener. Transm. Distrib. 17(2), 284–306 (2023). https://doi.org/10.1049/gtd2.12430
7. Grid-forming capabilities: Towards system level integration. ENTSO-E, Technical Document. https://www.entsoe.eu/news/2021/04/01/grid-forming-capabilities-ensuring-system-stability-with-a-high-share-of-renewables/ (2021). Accessed 21 Dec 2023
8. High penetration of power electronic interfaced power sources and the potential contribution of grid forming converters. ENTSO-E Technical Group on High Penetration of Power Electronic Interfaced Power Sources, Technical Report. https://www.entsoe.eu/Documents/Publications/SOC/High_Penetration_of_Power_Electronic_Interfaced_

Power_Sources_and_the_Potential_Contribution_of_Grid_Forming_Converters.pdf (2020). Accessed 21 Dec 2023
9. Lin, Y., et al.: Pathways to the next-generation power system with inverter-based resources: Challenges and recommendations. IEEE Electrific. Mag. 10(1), 10–21 (2022)
10. Expert Group: Advanced capabilities for grids with a high share of power park modules. GC-ESC, Technical Report. https://www.entsoe.eu/network_codes/cnc/expert-groups/ (2023). Accessed 21 Dec 2023
11. Recommendation No 03/2023 of the European Union Agency for the Cooperation of Energy Regulators. ACER. https://www.acer.europa.eu/news-and-events/news/acer-proposes-amendments-electricity-grid-connection-network-codes (2023). Accessed 21 Dec 2023
12. Roscoe, A., et al.: Response of a grid forming wind farm to system events, and the impact of external and internal damping. IET Renew. Power Gener. 14(19), 3908–3917 (2020)
13. Duckwitz, D., Knobloch, A., Welck, F., Becker, T., Gloeckler, C., Buelo, T.: Experimental short-circuit testing of grid-forming inverters in microgrid and interconnected mode. In: NEIS 2018, Conference on Sustainable Energy Supply and Energy Storage Systems, pp. 1–6. IEEE, Piscataway (2018)
14. Venkataramanan, A., Wang, W., Ramasubramanian, D., Huque, A., Key, T., Mehrizi-Sani, A.: Grid-forming distributed energy resources: Value in high renewable penetration and weak grid scenarios. In: Conference Proceedings of the 22nd Wind Solar Integration Workshop. IEEE, Piscataway (2023)
15. Li, C., Yang, Y., Cao, Y., Wang, L., Blaabjerg, F.: Frequency and voltage stability analysis of grid-forming virtual synchronous generator attached to weak grid. IEEE J. Emerg. Sel. Top Power Electron. 10(3), 2662–2671 (2022)
16. Rosso, R., Engelken, S., Liserre, M.: On the implementation of an FRT strategy for grid-forming converters under symmetrical and asymmetrical grid faults. IEEE Trans. Ind. Appl. 57(5), 4385–4397 (2021)
17. Schöll, C., Lens, H.: Instability phenomena in interconnected power systems caused by current limitation of grid-forming converters. In: Conference Proceedings of the 19th Wind Integration Workshop. IEEE, Piscataway (2020)
18. Schöll, C., Lens, H.: Impact of current limitation of grid-forming voltage source converters on power system stability. IFAC-PapersOnLine 53(2), 13520–13524 (2020)
19. Markovic, U., Stanojev, O., Aristidou, P., Vrettos, E., Callaway, D., Hug, G.: Understanding small-signal stability of low-inertia systems. IEEE Trans. Power Syst. 36(5), 3997–4017 (2021)
20. Frequency Stability in Long-Term Scenarios and Relevant Requirements. ENTSO-E Project Inertia Team, Technical Report. https://www.entsoe.eu/news/2021/12/06/entso-e-assesses-the-impact-of-reduction-of-inertia-on-frequency-stability-in-long-term-scenarios/ (2021). Accessed 21 Dec 2023
21. Ndreko, M., Rüberg, S., Winter, W.: Grid forming control scheme for power systems with up to 100% power electronic interfaced generation: a case study on Great Britain test system. In: IET Renewable Power Generation Special Issue: Wind and Solar Integration Workshop 2018, pp. 1268–1281. IET, Stevenage (2019)
22. Project MIGRATE – Massive InteGRATion of power Electronic devices: New Options in System Operations—Deliverable 3.4. https://www.h2020-migrate.eu/_Resources/Persistent/5d0f8339650bcf53cd24a3006556daa1da66cb42/D3.4%20-%20New%20Options%20in%20System%20Operations.pdf (2019). Accessed 4 Apr 2023
23. Laba, Y., Bruyère, A., Colas, F., Guillaud, X.: PQ decoupling on grid-forming converter connected to a distribution network. In: 2022 IEEE 13th International Symposium on Power Electronics for Distributed Generation Systems (PEDG), pp. 1–6. IEEE, Piscataway (2022). https://doi.org/10.1109/PEDG54999.2022.9923164
24. D'Arco, S., Suul, J.A.: Virtual synchronous machines—Classification of implementations and analysis of equivalence to droop controllers for microgrids. In Power Tech Grenoble, pp. 1–7. IEEE, Piscataway (2013)
25. D'Arco, S., Suul, J.A.: Equivalence of virtual synchronous machines and frequency-droops for converter-based microgrids. IEEE Trans. Smart Grid 5(1), 394–395 (2014)
26. Engler, A.: Device for parallel operation of equal range single- phase or three- phase voltage sources. Patent EP 1 286 444 B1 (2006)
27. Zhang, L.: Modeling and control of VSC-HVDC links connected to weak AC systems. Ph.D. Thesis, Royal Institute of Technology, School of Electrical Engineering, Stockholm (2010)
28. Laudahn, S., Seidel, J., Engel, B., Bulo, T., Premm, D.: Substitution of synchronous generator based instantaneous frequency control utilizing inverter-coupled DER. In: IEEE 7th International Symposium. IEEE, Piscataway (2016)
29. Schöll, C., Lens, H.: Design- and simulation-based comparison of grid-forming converter control concepts. In: Conference Proceedings of the 20th Wind Integration Workshop. IEEE, Piscataway (2021)
30. Sain, M., Massey, J.: Invertibility of linear time-invariant dynamical systems. IEEE Trans. Autom. Control 14(2), 141–149 (1969). https://doi.org/10.1109/TAC.1969.1099133
31. Yu, M., Roscoe, A.J., Booth, C.D., Dysko, A., Ierna, R., Zhu, J., Grid, N., Urdal, H.: Use of an inertia-less Virtual Synchronous Machine within future power networks with high penetrations of converters. In: Power Systems Computation Conference. IEEE, Piscataway (2016)
32. Kersic, M., Müller, T., Denninger, R., Ernst, P., Reichert, S., Singer, R., Dýsko, A., Egea Alvarez, A., Hong, Q., Lewis, E., Roscoe, A., Lens, H., Schöll, C., Schaupp, T., Jalili, K.: Testing characteristics of grid forming converters part I: Specification and definition of Behavior. In: Conference Proceedings of the 19th Wind Integration Workshop. IEEE, Piscataway (2020)
33. Denninger, R., Reichert, S., Rogalla, S., Jalili, K.: Testing characteristics of grid forming converters part II: voltage source properties and contribution to power quality. In: Conference Proceedings of the 19th Wind Integration Workshop. IEEE, Piscataway (2020)
34. Dýsko, A., Egea Alvarez, A., Hong, Q., Khan, A., Ernst, P., Singer, R., Roscoe, A.: Testing characteristics of grid forming converters part III: Inertial behavior. In: Conference Proceedings of the 19th Wind Integration Workshop. IEEE, Piscataway (2020)
35. Singer, R., Ernst, P., Denninger, R., Jalili, K.: Testing characteristics of grid forming converters part IV: Overload behavior and response to grid faults. In: Conference Proceedings of the 19th Wind Integration Workshop. IEEE, Piscataway (2020)
36. Valois-Rodriguez, M.F., Ungerland, J.: Evaluation of grid reduction techniques for distribution networks with a high penetration of inverter-based generation. In: 2020 IEEE PES ISGT-Europe, pp. 824–828. IEEE, Piscataway (2020)
37. Ungerland, J., Pant, P.: Challenges of modelling equivalent active distribution grids under consideration of grid forming inverters. In: Conference Proceedings of the 19th Wind Integration Workshop. IEEE, Piscataway (2020)
38. Ungerland, J., Poshiya, N., Biener, W., Lens, H.: A voltage sensitivity based equivalent for active distribution networks containing grid forming converters. IEEE Trans. Smart Grid 14(4), 2825–2836 (2022)
39. Amme, J., Pleßmann, G., Bühler, J., Hülk, L., Kötter, E., Schwaegerl, P.: The eGo grid model: An open-source and open-data based synthetic medium-voltage grid model for distribution power supply systems. In: Journal of Physics: Conference Series, vol. 977. Institute of Physics, London (2018)
40. Ernst, P., et al.: Verbundnetzstabil—Stabiles Verbundsystemverhalten bei umrichterbasierter Erzeugung: Schlussbericht: Forschungsprojekt 'Verbundnetzstabil. Freiburg (2022)

How to cite this article: Rogalla, S., Ernst, P., Lens, H., Schaupp, T., Schöll, C., Singer, R., Ungerland, J.: Grid-forming converters in interconnected power systems: Requirements, testing aspects, and system impact. IET Renew. Power Gener. 18, 3053–3066 (2024). https://doi.org/10.1049/rpg2.12967